

# On the Computation of Equilibrium Configurations of Elastically Coupled Nodes in Potential Fields

SILKE HANISCH, RENEE NÖLLE, THORSTEN BRANDT, THOMAS SATTEL

Heinz Nixdorf Institute  
Mechatronics and Dynamics  
University of Paderborn  
33102 Paderborn  
GERMANY

*Abstract-* Elastically coupled nodes exposed to artificial potential fields can be used as a model for path planning of autonomous mobile devices in unknown environments. In doing so, a possible path is provided by a spline interpolation of the nodes in their equilibrium positions. Repulsive potential fields are assigned to non-valid areas and moving obstacles identified by environmental sensors. In general the potential fields are nonlinear functions of position and time. Therefore, the equilibrium positions of the nodes can only be determined numerically. A modification of the Newton-Raphson method for this application is introduced and discussed with respect to its convergence properties. Finally, the method is illustrated by a simulation example.

*Key- Words:-* Newton-Raphson method, zero finding, path planning, autonomous systems, mobile robots

## 1 Introduction

To equip autonomous mobile devices with path planning capabilities in unknown environments is a great challenge with many technical applications, see [1], [2]. The proposed model of elastically coupled nodes is biologically inspired by insects using antennae to sense their environment, as motivated in Fig. 1. However, for path planning the environmental sensing of the antennae is extended by perception of motions of obstacles.

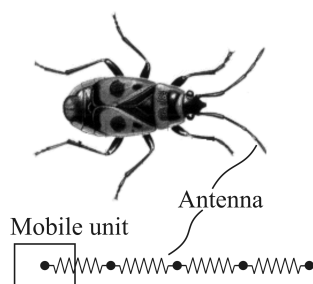


Fig. 1: Biological inspiration of virtual antennae modeling

Kinematic information of the environment is collected by sensors and incorporated in the external potentials acting on the nodes of the antennae. Appropriate repulsive potential fields are as-

signed to objects in the environment. Interpolation points of safe traveling paths for the autonomous device are provided by the equilibrium positions of the elastically coupled nodes exposed to external potentials. In general the external potentials are nonlinear, time depending functions of the position vectors. Therefore, the equilibrium configuration of the antennae can only be determined numerically. In this paper a particularly tailored Newton-Raphson method for this application is presented.

The setup of the antenna model exposed to external potentials is presented first. Subsequently, the Newton-Raphson method and the according modifications are discussed accounting for its convergence properties. The overall procedure is then demonstrated by a simulation example.

## 2 Model Setup

The mobile unit sketched in Fig. 2 may represent a mobile robot or any kind of ground vehicle. It is assumed that the mobile unit is capable of sensing positions and velocities of environmental obstacles and boundaries relative to itself. A virtual antenna, attached to the mobile unit, is

modeled by elastically coupled nodes  $P_i$ , where the coupling between adjacent nodes is realized by springs. Without environmental disturbances, the antenna stays in an undeformed equilibrium configuration aligned towards the planned direction of motion of the mobile unit. The node  $P_0$  is fixed to a reference point on the mobile unit while the node  $P_N$  is placed in the planned direction of motion at a distance corresponding to the maximum sensor detection range. Since the mobile unit is only allowed to navigate on collision-free paths, a potential field is assigned to each environmental boundary or obstacle detected by the sensor system of the mobile unit. As a consequence of these potential fields, repelling forces act on each node  $P_i$  transforming the antenna into a penetration free equilibrium configuration as shown in Fig. 2.

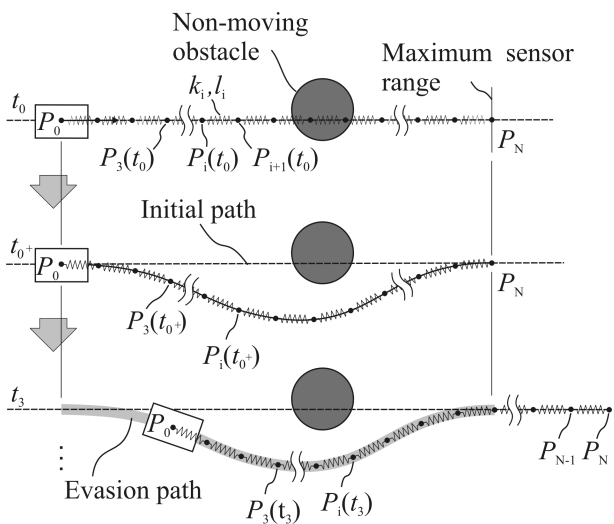


Fig. 2: Path planning procedure at times  $t_0, t_{0+}, t_3$

At time  $t_{0+}$ , shortly after  $t_0$ , a spline interpolation of the nodes  $P_i(t_{0+})$  is carried out to provide the evasion path. Figure 2 shows the position of the mobile unit with the attached antenna moving along the evasion path exemplary for the instant of time  $t_3$ . Note, that in the following, the instant of time  $t_i$  denotes the time, when the mobile unit would pass the position of node  $P_i(t_{0+})$ .

After this brief outline, the concept of motion planning using a virtual antenna is now presented in more detail. The idea of the proposed concept is based on the method of elastic bands, first introduced in [3] for robotic path planning. In [4] this method was applied to vehicle following problems.

Recently, [5] applied and extended this method to vehicle collision avoidance maneuver problems. In Fig. 3 an example of a complex environment is shown.

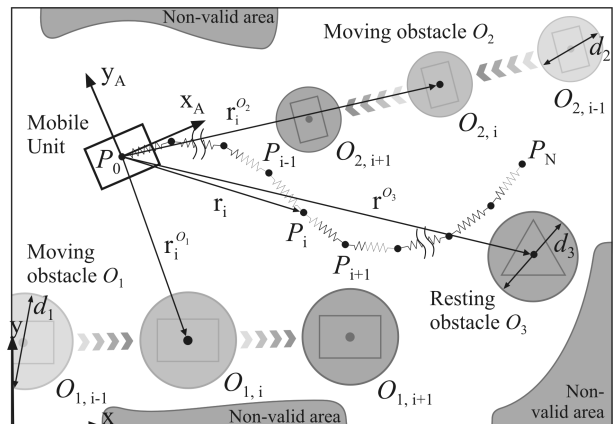


Fig. 3: Mobile unit navigating in a complex environment with the global reference frame  $(x, y)$  and the mobile unit fixed reference frame  $(x_A, y_A)$

For the method outlined here, it is assumed that the mobile unit moves with a given speed  $v(t)$ . The position vector  $\mathbf{r}_i^{O_j} := \mathbf{r}^{O_j}(t_i)$  of an obstacle  $O_j$  at time  $t_i$  and the position vector  $\mathbf{r}_i$  of a node  $P_i$  of the antenna are represented in a reference frame  $(x_A, y_A)$ . Points on the path of a moving obstacle  $O_j$  at the instance of time  $t_i$  are denoted by  $O_{j,i} := O_j(t_i)$ . As a simplification of the geometry of the obstacles  $O_j$  a safety circle of diameter  $d_j$  is chosen. By assuming constant velocity of moving obstacles during the planned evasion maneuver, the path of a moving obstacle is linearly extrapolated, see the paths  $O_{j,i-1}, O_{j,i}, O_{j,i+1}$ ,  $j \in \{1, 2\}$  in Fig. 3. The mobile unit plans to move along the initial path at the given velocity  $v(t)$  starting from the position at node  $P_0$  at time  $t_0$ . At time  $t_i$ , the mobile unit would pass the position of node  $P_i$ . At the same time  $t_i$ , the obstacles would occupy the positions of the nodes  $O_{j,i}$ ,  $j \in \{1, 2\}$ .

Each node  $P_i$  of the antenna is influenced by the internal potential

$$V_i^{\text{int}} = \frac{1}{2}k_i(\|\mathbf{r}_{i+1} - \mathbf{r}_i\| - l_i)^2 + \frac{1}{2}k_{i-1}(\|\mathbf{r}_i - \mathbf{r}_{i-1}\| - l_{i-1})^2 \quad (1)$$

of its adjacent springs  $i$  and  $i - 1$ . Therein  $l_i$  denotes the initial length and  $k_i$  the stiffness of spring  $i$ , respectively, see Fig. 2. The internal force  $\mathbf{F}_i^{\text{int}}$  acting on node  $P_i$  is given by the directional

derivative of the potential of the springs evaluated at  $P_i$

$$\begin{aligned} \mathbf{F}_i^{\text{int}} &= -\frac{\partial V_i^{\text{int}}}{\partial \mathbf{r}_i} \\ &= k_i(\|\mathbf{r}_{i+1} - \mathbf{r}_i\| - l_i) \frac{\mathbf{r}_{i+1} - \mathbf{r}_i}{\|\mathbf{r}_{i+1} - \mathbf{r}_i\|} \\ &\quad - k_{i-1}(\|\mathbf{r}_i - \mathbf{r}_{i-1}\| - l_i) \frac{\mathbf{r}_i - \mathbf{r}_{i-1}}{\|\mathbf{r}_i - \mathbf{r}_{i-1}\|}. \end{aligned} \quad (2)$$

The external potential at the node  $P_i$

$$V_i^{\text{ext}} := V^{\text{ext}}(\mathbf{r}_i, t_i) = V^B(\mathbf{r}_i) + \sum_j V^{O_j}(\mathbf{r}_i, t_i) \quad (3)$$

is made up from the external potential fields of the environmental boundaries  $V_i^B := V^B(\mathbf{r}_i)$  and the time dependent potential fields  $V_i^{O_j} := V^{O_j}(\mathbf{r}_i, t_i)$  of the obstacles  $O_j$  at time  $t_i$ . For the particular scenario, shown in Fig. 3, the external potential field  $V^{\text{ext}}((x, y), t_i)$ ,  $(x, y) \in \mathbb{R}^2$ , virtually sensed by node  $P_i$  at time  $t_i$  is illustrated in Fig. 4.

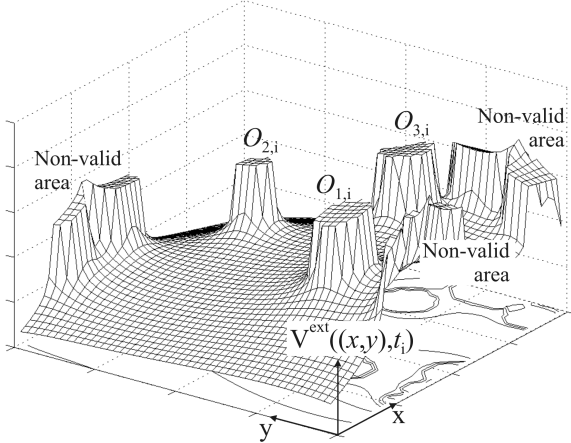


Fig. 4: Potential field of the complex environment in Fig. 3 sensed by node  $P_i$  at  $t_i$

Now, the influence of the external potential  $V_i^{\text{ext}}$  on each node  $P_i$  of the antenna is addressed. The potentials of obstacles act between positions of the mobile unit and of the obstacles that would be occupied at the same time. By taking the directional derivatives of the external potentials with respect to a node  $P_i$  the external force acting on the node  $P_i$  is given by

$$\mathbf{F}_i^{\text{ext}} := F^{\text{ext}}(\mathbf{r}_i, t_i) = -\frac{\partial V_i^{\text{ext}}}{\partial \mathbf{r}_i}. \quad (4)$$

Thus, a node close to a non-valid area is repulsed. The external forces on node  $P_i$  of the antenna due to the potential fields of the obstacles and the environmental boundaries is illustrated in Fig. 5.

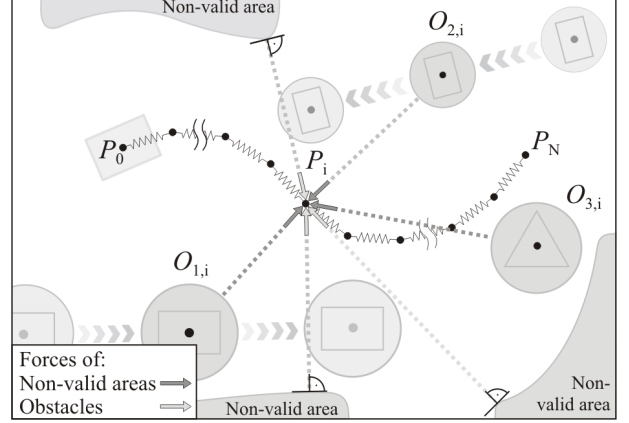


Fig. 5: External forces acting on node  $P_i$  at  $t_i$ .

Force equilibrium

$$\mathbf{F}_i^{\text{sum}} = \mathbf{F}_i^{\text{ext}} + \mathbf{F}_i^{\text{int}} = 0, \quad i = 0, \dots, N. \quad (5)$$

at each node  $P_i$  of the antenna gives the equilibrium solution in the deformed configuration.

To detect different possibilities to evade obstacles, first approximations of solution paths are needed. If more than one equilibrium solution exist, it should be ensured that all start configurations of the antenna migrate into different equilibria. After smoothing the resulting equilibrium solutions by interpolation with cubic splines, the evasion path has to be selected. Therefore, certain selection criteria are conceivable. One example is given in section 4.

In general (5) represents a nonlinear system of equations of several variables that can only be solved numerically. The complexity of the calculation of a solution of (5) depends on the geometry of the non-valid areas as well as on the number of obstacles and their behavior.

### 3 Numerical Procedure

The problem of finding roots of a given function  $\mathbf{F} : \mathbb{R}^n \rightarrow \mathbb{R}^n$  may be written in the form

$$\mathbf{F}(\mathbf{x}) = \mathbf{0}. \quad (6)$$

A popular approach for solving (6) is known as Newton-Raphson method.

### 3.1 The Newton-Raphson method

The Newton-Raphson iteration can be interpreted as a linear approximation

$$\mathbf{F}(\mathbf{x}) \simeq \tilde{\mathbf{F}}(\mathbf{x}) := \mathbf{F}(\mathbf{x}^n) + \mathbf{J}(\mathbf{x}^n)(\mathbf{x} - \mathbf{x}^n), \quad (7)$$

obtained by truncating the Taylor series expansion of  $\mathbf{F}$  at  $\mathbf{x}^n$  after the linear term and then solving the resulting linear equation  $\tilde{\mathbf{F}}(\mathbf{x}) = \mathbf{0}$ , calling the solution  $\mathbf{x}^{n+1}$  ([7], p.181-185). The matrix  $\mathbf{J}$  denotes the Jacobian of  $\mathbf{F}$ . Performing an iteration step, (7) leads to

$$\mathbf{x}^{n+1} = \mathbf{x}^n - \mathbf{J}^{-1}(\mathbf{x}^n)\mathbf{F}(\mathbf{x}^n), \quad n = 0, 1, 2, \dots \quad (8)$$

At best, starting from an initial vector  $\mathbf{x}^0$  the approximation converges to a root  $\mathbf{x}^*$ .

In many cases, solutions of nonlinear equations can be approximated by considering a fixed point problem: Find  $\mathbf{x} \in R^n$  such that for the mapping  $\phi : R^n \rightarrow R^n$

$$\phi(\mathbf{x}) = \mathbf{x} \quad (9)$$

holds. By choosing

$$\phi(\mathbf{x}) := \mathbf{x} - \mathbf{J}^{-1}(\mathbf{x})\mathbf{F}(\mathbf{x}) \quad (10)$$

the fixed point iteration

$$\mathbf{x}^{n+1} = \phi(\mathbf{x}^n), \quad n = 0, 1, 2, \dots \quad (11)$$

also known as the Banach-Iteration, generates a sequence of approximations described in (8) being the Newton-Raphson iteration for solving  $\mathbf{F}(\mathbf{x}) = \mathbf{0}$ . Therefore, the convergence criteria of the Banach-Iteration (11) are also valid for the special case of the Newton-Raphson method. Hence, the Newton-Raphson method converges to a root  $\mathbf{x}^*$  if the requirements of the fixed point theorem are met in a sufficiently small neighborhood of the root  $\mathbf{x}^*$  ([6], p.305-307, [7], p.311). In this context the function  $\phi : R^n \rightarrow R^n$  has to be contractive

$$\|\phi(\mathbf{x}_i) - \phi(\mathbf{x}_j)\| \leq k\|\mathbf{x}_i - \mathbf{x}_j\|, \quad \forall \mathbf{x}_i, \mathbf{x}_j \in R^n \quad (12)$$

with a contraction constant  $k \in [0, 1)$ , that can be estimated by the spectral radius  $\rho(\phi'(\mathbf{x}^*))$  ([6], p.169, 299-304, [7], p.311).

### 3.2 Modifications of the Newton-Raphson method for path planning

Applying the Newton-Raphson iteration to the nonlinear system (5), leads to

$$\mathbf{r}^{n+1} = \mathbf{r}^n - \mathbf{J}^{-1}(\mathbf{r}^n)\mathbf{F}(\mathbf{r}^n), \quad n = 0, 1, 2, \dots \quad (13)$$

where  $\mathbf{r}^n := [\mathbf{r}_0^n, \dots, \mathbf{r}_N^n]$  consists of all position vectors  $\mathbf{r}_i^n$  of the nodes at the  $n^{\text{th}}$  iteration step. The initial configuration of the antenna is denoted by the vector  $\mathbf{r}^0$ .

As pointed out in section 2, the force vector  $\mathbf{F}$  and therefore the Jacobian matrix  $\mathbf{J}$  do not only depend on the positions of the nodes  $P_i$  but also on the corresponding instances of time  $t_i$ . So (13) may be written as

$$\begin{aligned} \mathbf{r}^{n+1} &= \mathbf{r}^n - \mathbf{J}^{-1}(\mathbf{r}^n, \mathbf{t}^n)\mathbf{F}(\mathbf{r}^n, \mathbf{t}^n) \\ \Rightarrow \mathbf{J}(\mathbf{r}^n, \mathbf{t}^n)\Delta\mathbf{r}^{n,n+1} &= -\mathbf{F}(\mathbf{r}^n, \mathbf{t}^n) \quad (14) \\ n &= 0, 1, 2, \dots \end{aligned}$$

where the vector  $\mathbf{t}^n := [t_0^n, \dots, t_N^n]$  consists of the instances of time  $t_i$ ,  $i = 0, \dots, N$ , and  $\Delta\mathbf{r}^{n,n+1} = \mathbf{r}^{n+1} - \mathbf{r}^n$  defines the displacement vector of the antenna in the  $n^{\text{th}}$  iteration step, respectively. Note that at each iteration step  $n$  the instances of time at which the displaced nodes would be passed through are changed, such that in each subsequent iteration step the positions  $\mathbf{r}_i^{O_j}$  of the obstacles have to be evaluated again.

In case the absolute value of the displacement vector  $\Delta\mathbf{r}^{n,n+1}$  and therefore the changes in the positions of the nodes decay with increasing number of iteration steps it is guaranteed that the differences in time and thereby the differences in the positions of the obstacles decrease, too. Thus, the convergence of the modified time dependent procedure is dominated by the convergence behavior of the Newton-Raphson method.

The external potential fields, as for example depicted in Fig. 4, are defined in a way such that their gradients are directed towards the valid area. This ensures the existence of minima inside the valid area. Thus, the problem of finding roots of the gradient mapping of a potential field can be solved by the Newton-Raphson method. To prevent that a node of the antenna drops out of the valid area constraints for the vector of displacement  $\Delta\mathbf{r}^{n,n+1}$  are formulated. In case that

in one iteration step  $\tilde{n}$  the vector  $\Delta \mathbf{r}_i^{\tilde{n}, \tilde{n}+1}$  shifts a node  $P_i$  into a non-valid area, it is cut to the half length of the shortest distance to the corresponding boundary,  $\Delta \mathbf{r}_i^{\tilde{n}, \tilde{n}+1} \rightarrow \Delta \bar{\mathbf{r}}_i^{\tilde{n}, \tilde{n}+1}$ , as shown in Fig. 6.

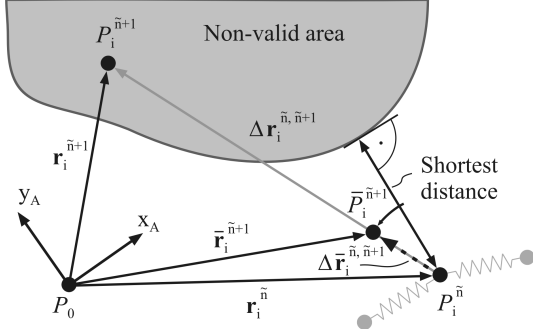


Fig. 6: Restriction of the iteration to valid solution spaces.

In doing so, it is ensured that the nodes permanently remain in the valid area for all iteration steps of the Newton-Raphson iteration.

The internal forces of the antenna influence the position of the nodes locally. It is desired that the nodes migrate into collision-free configurations which do not twist and have no peaks. Starting with an inner spring stiffness being too low the antenna may start to build out peaks or to twist. Twisting means that in one iteration step some nodes of the antenna pass each other. Here, higher stiffness between the effected nodes are practical. Otherwise for spring stiffness being too high the flexibility of the antenna is restricted, such that the equilibrium configuration eventually still intersects the path of an obstacle. In the latter case it is necessary to recheck the collision risk and if need is to scale down the inner spring stiffness for all intervals.

In order to detect all possible equilibrium configurations of the antenna in the potential field it is also useful to turn off the internal spring forces at certain nodes temporally.

#### 4 Simulation Example

As already mentioned, the number of equilibrium solutions of the antenna is not restricted to a single one. However, for locomotion a desired path has to be selected with respect to a relevant criterion depending on the application. For energy

critical systems the path that can be followed with minimal energy effort

$$E(\mathbf{u}, t) = \int_{t_{start}}^{t_{end}} \mathbf{u}(\tau) d\tau \quad (15)$$

may be chosen, where  $\mathbf{u}$  denotes the control vector keeping the mobile unit on the prescribed path. For devices traveling at high velocities the lateral acceleration

$$a_n = v^2(t)\kappa, \quad (16)$$

where  $\kappa$  denotes the curvature, experienced on the considered path, may be a suitable selection criterion.

Fig. 7 illustrates the results of a sample simulation scenario. A mobile unit moves at a constant velocity of  $30 \frac{m}{s}$  on a rectangular 7m wide corridor. At time  $t_0$  a resting obstacle appears 65m ahead. A second oncoming obstacle travels from an initial distance of 55m at a speed of  $20 \frac{m}{s}$ . The influence of the borders of the corridor as well as of the obstacles is modeled by logarithmic potentials. The potential  $V_i^{O_j}$  of obstacle  $O_j$  evaluated at node  $P_i$  is defined as

$$V_i^{O_j} = -k^{O_j} \ln(\|r_i - r_i^{O_j}\| - \frac{d_j}{2}), \quad (17)$$

where  $k^{O_j}$  and  $d_j$  denote the scaling factor of the obstacle and its safety circle, respectively. To evaluate the external potential of the borders of the corridor at node  $P_i$  reference points at the borders, given by the vector  $r_i^{B_{l,r}}$  are assigned to each node  $P_i$ . The potential of the borders  $V_i^{B_{l,r}}$  evaluated at node  $P_i$  is determined separately for the left and the right border by

$$V_i^{B_{l,r}} = -k^{B_{l,r}} \ln(\|r_i - r_i^{B_{l,r}}\|). \quad (18)$$

In Fig. 7 the positions of the obstacles symbolized by their safety circles as well as the position of the mobile unit are depicted over the entire planned time period  $[t_{0+}, t_N]$ .

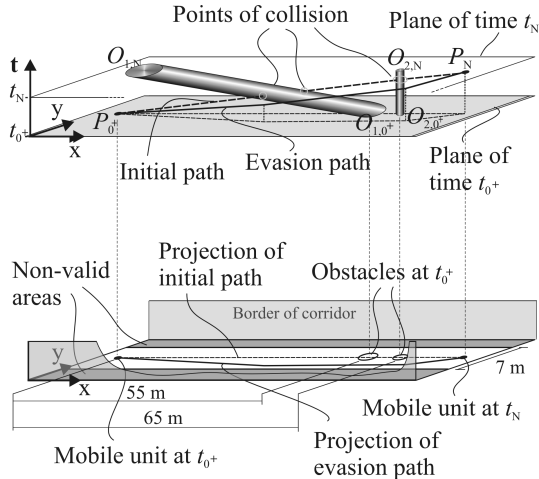


Fig. 7: Spatial-temporal representation of the simulation result

Therefore, cylinders are formed with the time being the third dimension. Possible collision points resulting from the initial configuration of the antenna are indicated. The path planning parameters are summarized in Tab. 1.

The evasion path, shown in Fig. 7, was calculated by use of the modified Newton-Raphson method in 45 iteration steps with an accuracy of  $\epsilon = 0.05$ . The stiffness of the internal springs remained unchanged over the iteration. In the final configuration the spectral radius was evaluated to  $k = 0.4712$  underlining the good conditioning of the procedure and therefore a posteriori approving convergence ([7], p.300-311, [6], p.158-162).

Tab. 1: Path planning parameters

Symbol	Description	Value	Unit
$k_i$	Initial internal spring stiffness of all springs $i$	10000000	[-]
$k^{B_r}$	Force scaling factor of the right border	1/3	[-]
$k^{B_l}$	Force scaling factor of the left border	1	[-]
$k^{O_1}$	Force scaling factor, oncoming obstacle	1	[-]
$k^{O_2}$	Force scaling factor, resting obstacle	1	[-]
$d_1$	Safety diameter, oncoming obstacle	4	[m]
$d_2$	Safety diameter, resting obstacle	2	[m]
$l_i$	Initial length of all internal springs $i$	0.404	[m]
$n$	Number of nodes	100	[-]

## 5 Conclusion

A model of elastically coupled nodes, biologically inspired by antennae of insects, was presented as an approach to path planning problems of autonomous devices. To determine the solution path given by an interpolation of the equilibrium positions of the nodes, exposed to external potentials, the Newton-Raphson method was modified. The modifications force the iteration procedure to stay inside valid areas of the environment and avail convergence because the nodes are kept in heuristically known areas including the equilibrium positions. The application of the method was demonstrated in a simulation example.

## References

- [1] Stadler, Wolfram (1995). *Analytical Robotics and Mechatronics*. McGraw-Hill Inc., Series in Electrical and Computer Engineering
- [2] Consolini, L., Piazzini, A., Tosques, M. (2001). *Motion planning for steering car-like vehicles*, Proceedings of the European Control Conference, pp. 1834-1839.
- [3] Quinlan, S. and Khatib, O. (1993). *Elastic Bands: Connecting Path Planning and Control*. IEEE International Conference on Robotics and Automation, vol. 2, pp. 802-807, Atlanta (GA), USA
- [4] Gehring, S.K. and Stein, F.J. (2001). *Elastic Bands to Enhance Vehicle Following*. IEEE Intelligent Transportation Systems Conference Proceedings, Oakland (CA), USA
- [5] Brandt, T., Sattel, T., Wallaschek, J. (2004). *On automatic collision avoidance*, Proceedings 21. VDI/VW Conference, Integrated Safety and Driver Assistance Systems, 27.-28. October 2004, Wolfsburg, Germany, (in German)
- [6] Oevel, Walter (1996). *Einführung in die Numerische Mathematik*. Spektrum Akademischer Verlag GmbH, Heidelberg
- [7] Ortega, J.M., Rheinboldt, W.C. (1970). *Iterative Solution of Nonlinear Equations in Several Variables*. Academic Press, New York